

See discussions, stats, and author profiles for this publication at: <https://www.researchgate.net/publication/269182817>

Carbon Dioxide Capture with the Ozone-like Polynitrogen Molecule Li_3N_3

ARTICLE in THE JOURNAL OF PHYSICAL CHEMISTRY A · DECEMBER 2014

Impact Factor: 2.69 · DOI: 10.1021/jp509933x · Source: PubMed

READS

41

2 AUTHORS, INCLUDING:



Antonio J. C. Varandas

University of Coimbra

382 PUBLICATIONS 6,750 CITATIONS

SEE PROFILE

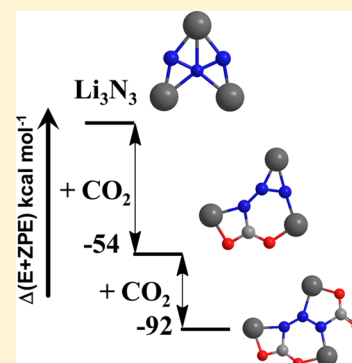
Carbon Dioxide Capture with the Ozone-like Polynitrogen Molecule Li_3N_3

Miquel Torrent-Sucarrat* and António J. C. Varandas*

Departamento de Química and Centro de Química, Universidade de Coimbra, 3004-535 Coimbra, Portugal

S Supporting Information

ABSTRACT: In a very recent article (*Chem.—Eur. J.* **2014**, *20*, 6636), Olson et al. performed a theoretical study of the low-lying isomers of Li_3N_3 and found that two of the most stable structures show a novel N_3^{3-} molecular motif, which possesses structural and chemical bonding features similar to ozone. We explore a first application of these new Li_3N_3 species as a captor of carbon dioxide. Our results conclude that this is a very exothermic and exoergic process (the capture of one and two carbon dioxide molecules on Li_3N_3 releases, respectively, 42 and 70 kcal mol⁻¹ in relative free energy values evaluated at the CCSD(T)/aug-cc-pVTZ//B3LYP/aug-cc-pVTZ level of theory), which apparently occurs without any energy barrier but requires a nonlinear N_3^{3-} molecular motif.



1. INTRODUCTION

Carbon dioxide, CO_2 , is one of the main greenhouse gases in the Earth's atmosphere, i.e., a gas that absorbs the thermal infrared radiation from the Earth's surface and re-emits it in all directions (surface and lower atmosphere). The Earth's natural greenhouse effect increases the average surface temperature around 33 °C and makes possible life as we know it. The CO_2 emission from combustion of fossil fuels intensifies the natural greenhouse effect, causing the main source of global climate change through global warming.^{1–4} The search for methods that can capture and isolate CO_2 has therefore become one of the grand challenges of the 21st century. For instance, several attempts have been reported to transform carbon dioxide into hydrocarbons among others (formaldehyde, methanol, formic acid, etc.) through chemical reactions and electrochemical reductions.^{5–13}

Of the different methodologies to adsorb and separate CO_2 , the procedures where a nitrogen atom is used to capture the carbon dioxide have started to be broadly employed, e.g., ionic liquids and amine solutions, mainly monoethanolamine, react with carbon dioxide, yielding carbamates.^{14–16} Luo et al.¹⁷ proposed a pyridine containing anion functionalized ionic liquid capable of capturing CO_2 in a reversible way through multiple-site cooperative interactions. As we can see, the synthesis of novel molecules and materials with nitrogen atoms results in being key for the research of new CO_2 capture procedures. Another possibility is the use of polynitrogen systems, although they result in being very difficult to synthesize; e.g., only two years ago the first alkali diazine Li_2N_2 was obtained by decomposition of LiN_3 under high pressure and temperature conditions.¹⁸ In this regard, computational chemistry can be a powerful tool to guide the search for new polynitrogen materials.

Olson et al.¹⁹ studied from a theoretical point of view the 14 low-lying isomers of Li_3N_3 . Among the four more stable isomers, they report two structures (the third and fourth lowest lying conformers) with a novel N_3^{3-} molecular motif, which possesses structural and chemical bonding features similar to ozone. Olson et al. considered that this lithium triazenide Li_3N_3 can be produced under rather specific experimental conditions, even containing the nonlinear ozone-like N_3^{3-} molecular motif. It is worth noting that the synthesis of the Li_3N_3 system will be a complicated and challenging, but available, process, and in a similar way to the novel synthetic approach of the crystal structure of Li_2N_2 ¹⁸ it will require high pressure and high temperature conditions. The aim of this work is to suggest a first application of such a Li_3N_3 species as a captor of CO_2 .

In a highlight article of CO_2 fixation, Schulz and co-workers²⁰ were surprised that CO_2 complexes with small nucleophilic anions, such as halides or pseudohalides (e.g., OH^- , CN^- , OCN^- , SCN^- , and N_3^-), have not been thoroughly studied to date. Exceptions are the following three cases: the well-known bicarbonate ion, $[\text{OHCO}_2]^-$, fluorocarbonate ion $[\text{FCO}_2]^-$,²¹ and the recent cyanofornate ion $[\text{NCCO}_2]^-$ reported by Murphy et al.²² The latter is particularly interesting because its stability is dependent on the dielectric constant of the local environment (a polarity switchable solvent): it is stable in low polarity systems and unstable in high-polarity adducts, releasing carbon dioxide. Reversibility of the CO_2 capture is essential to warrant an effective method to reduce the non-natural greenhouse effect; the cyanofornate ion is a promising example of a CO_2 complex which can be formed or destroyed on

Received: October 2, 2014

Revised: December 3, 2014

Published: December 3, 2014

demand with Lewis bases by changing the solvent.^{22,23} As far as we know, the only other exception that can be considered from a theoretical point of view is the work by Varandas,²⁴ who predicts the $\text{Li}_3\text{N} + \text{CO}_2$ reaction to form Li_3NCO_2 in a process without any apparent energy barrier and highly exothermic: $-84.5 \text{ kcal}\cdot\text{mol}^{-1}$ at the CCSD(T)/aug-cc-pVTZ level of theory. This work can also be considered according to the words of Schulz and co-workers²⁰ as another example of CO_2 capture by a nucleophilic anion, N_3^{3-} .

2. COMPUTATIONAL METHODS

All calculations have been carried out with the Gaussian09 program package.²⁵ They use the Kohn–Sham density functional method with the B3LYP,²⁶ M06-2X,²⁷ and CAM-B3LYP²⁸ functionals and the cc-pVTZ and aug-cc-pVTZ basis sets.^{29–31} The simplest of these basis sets has been used for exploratory purposes, while the aug-cc-pVTZ one is utilized to obtain the final results. At this level of theory, we have also calculated the harmonic frequencies to verify the nature of the stationary points and provide the zero-point vibrational energy (ZPE) as well as the thermodynamic contribution to the enthalpy and free energy at 298 K. With the aim to get more accurate relative energies, we have performed CCSD(T)^{32–34} calculations at the optimized geometries using the aug-cc-pVTZ basis set. Of course, a caution point has to be made since recent work^{35–37} has shown that “model chemistries” using hybrid methodologies may be misleading in describing the topography of the potential energy surfaces described by the pure “chemistries” involved. This does not appear though to have severe consequences in the present work. The fuzzy atom bond orders³⁸ using the atomic definition of the Becke-rho scheme^{39,40} have been evaluated with the FUZZY program.⁴¹ We should also note that the optimized structures have been restricted to the symmetry suggested by the optimization process, with the Cartesian coordinates of all minima so obtained available as Supporting Information.

3. RESULTS AND DISCUSSION

The four lowest lying structures of Li_3N_3 reported by Olson et al.¹⁹ with the most relevant geometrical parameters are displayed in Figure 1. Structures I, II, and IV show C_{2v} symmetry, while III is of the C_s type. In the isomers III and IV, the N_3^{3-} molecular motif is nonlinear and possesses structural and chemical bonding features similar to ozone. Conversely, I and II are linear. Table 1 collects the energetic results obtained in this work at the B3LYP/aug-cc-pVTZ and CCSD(T)/aug-cc-pVTZ//B3LYP/aug-cc-pVTZ levels of theory. Also given are the relative energies accounting for the zero-point vibrational energy corrections, $\Delta(E+\text{ZPE})$, at the CCSD(T)/6-311++G(d,p)//CCSD(T)/6-311++G(d,p) level from the work of Olson et al.¹⁹ It is worth noting that in all three levels of theory the most stable conformation is I. At the B3LYP level, the four lowest lying structures are almost isoenergetic (the difference between isomers is not larger than $2.5 \text{ kcal}\cdot\text{mol}^{-1}$, $\Delta(E+\text{ZPE})$ values). Regarding the CCSD(T) benchmarking results, the linear structures (I and II) are more stable by about $5 \text{ kcal}\cdot\text{mol}^{-1}$ than the nonlinear conformations (III and IV). We have also evaluated their relative stability using the M06-2X/aug-cc-pVTZ and CAM-B3LYP/aug-cc-pVTZ methods (see the Supporting Information), with the results being somewhat poorer in comparison to the CCSD(T) ones

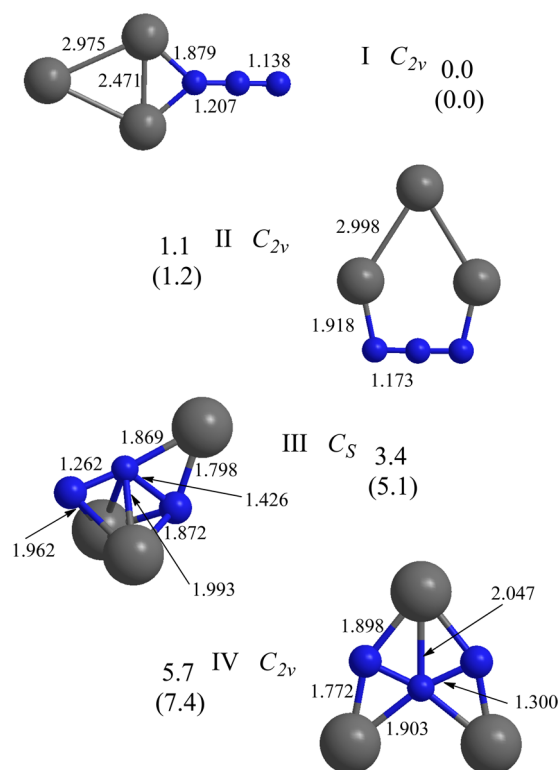


Figure 1. Four lowest-lying structures of Li_3N_3 evaluated at the CCSD(T)/aug-cc-pVTZ//B3LYP/aug-cc-pVTZ level of theory. The values are relative energies plus ZPE, with relative free energies given in brackets, all in $\text{kcal}\cdot\text{mol}^{-1}$.

Table 1. Relative Energies, Energies plus ZPE, Enthalpies, and Free Energies (in $\text{kcal}\cdot\text{mol}^{-1}$ at 298 K) Calculated for the Four Lowest Lying Isomers of Li_3N_3 .

compd	$\Delta(E+\text{ZPE})^a$	ΔE^b	ΔE^c	$\Delta(E+\text{ZPE})^c$	ΔH^c	ΔG^c
I	0.0	0.0	0.0	0.0	0.0	0.0
II	1.2	2.8	1.3	1.1	1.2	1.2
III	6.2	0.6	3.4	3.4	2.4	5.1
IV	8.1	0.0	5.6	5.7	4.9	7.4

^aRelative energies plus ZPE correction computed at the CCSD(T)/6-311++G(d,p)//CCSD(T)/6-311++G(d,p) level of theory from ref 19.

^bEnergies computed at the B3LYP/aug-cc-pVTZ level of theory.

^cEnergies computed at the CCSD(T)/aug-cc-pVTZ//B3LYP/aug-cc-pVTZ level of theory from this work. ZPE and enthalpic and entropic corrections correspond to calculations at the B3LYP/aug-cc-pVTZ level of theory.

than those based on B3LYP, e.g., the conformer III is the most stable one at the M06-2X and CAM-B3LYP levels.

In a similar way to the $\text{Li}_3\text{N} + \text{CO}_2$ reaction,²⁴ the carbon dioxide capture by Li_3N_3 occurs promptly (without any apparent energy barrier). For more details, see Figure S1 in the Supporting Information with relaxed potential energy surface scans along the N– CO_2 distance for the $\text{Li}_3\text{N}_3\text{CO}_2$ and $\text{Li}_3\text{N}_3(\text{CO}_2)_2$ compounds investigated in the present work. For this reason, the exploration of the potential energy surface of $\text{Li}_3\text{N}_3 + \text{CO}_2$ has been done by locating the carbon dioxide at about 2 \AA from each nitrogen atom of the four lowest-lying structures of Li_3N_3 , while considering also different orientations for CO_2 with respect to Li_3N_3 . Then, the system was optimized, and only the structures showing the carbon dioxide bonded to the N_3^{3-} molecular motif have been selected and displayed in

Figure 2 together with their most relevant geometrical parameters. The results regarding their relative stabilities with respect to the isolated reactants are collected in Table 2.

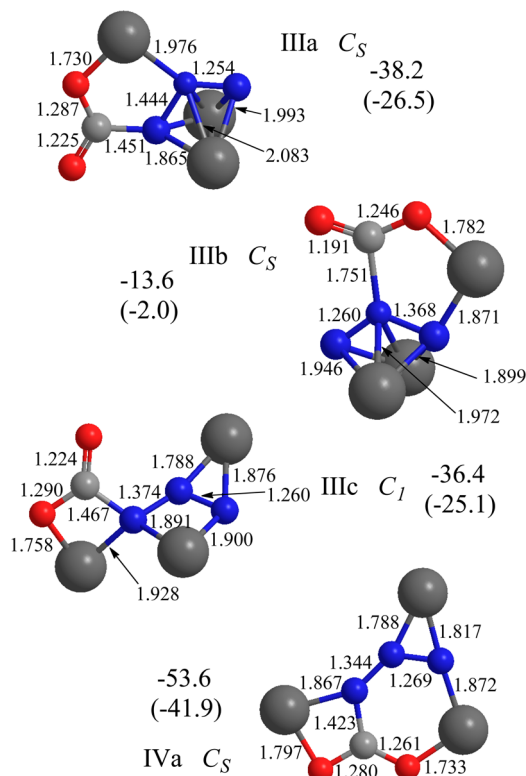


Figure 2. Structures of the organic compounds obtained from the interaction of the four lowest-lying structures of Li_3N_3 (see Figure 1) with CO_2 evaluated at the CCSD(T)/aug-cc-pVTZ//B3LYP/aug-cc-pVTZ level of theory. The values are relative energies plus ZPE, with relative free energies given in parentheses, all in kcal mol^{-1} .

Table 2. Relative Energies, Energies plus ZPE, Enthalpies, and Free Energies (in kcal mol^{-1} at 298 K) Calculated for the Organic Compounds Obtained from $\text{Li}_3\text{N}_3 + \text{CO}_2$ and $\text{Li}_3\text{N}_3 + 2\text{CO}_2$

compd	ΔE^a	ΔE^b	$\Delta(E+ZPE)^b$	ΔH^b	ΔG^b
Li_3N_3 (I) + CO_2	0.0	0.0	0.0	0.0	0.0
IIIa	-37.4	-40.1	-38.2	-39.9	-26.5
IIIb	-15.4	-15.5	-13.6	-15.2	-2.0
IIIc	-36.7	-38.3	-36.4	-37.8	-25.1
IVa	-57.3	-56.3	-53.6	-55.3	-41.9
Li_3N_3 (I) + 2CO_2	0.0	0.0	0.0	0.0	0.0
IIIaa	-55.2	-62.9	-59.4	-61.5	-36.9
IVaa	-77.7	-81.3	-76.8	-79.1	-54.9
IVab	-92.3	-96.7	-92.2	-94.5	-70.3

^aEnergies computed at the B3LYP/aug-cc-pVTZ level of theory.

^bEnergies computed at the CCSD(T)/aug-cc-pVTZ//B3LYP/aug-cc-pVTZ level of theory. ZPE and enthalpic and entropic corrections correspond to calculations at the B3LYP/aug-cc-pVTZ level of theory.

It is worth noting that the CO_2 interaction with the linear N_3^{3-} molecular motif is not possible, with the carbon dioxide remaining at about 3 Å distant, thus forming a van der Waals complex with I and II. On the other hand, with the ozone-like N_3^{3-} , four $\text{Li}_3\text{N}_3\text{CO}_2$ compounds can be created (see Figure 2). The structures IIIa, IIIb, and IIIc are obtained from the isomer

III of Li_3N_3 , whereas IVa is generated from IV. The relative stability of these systems with respect to the isolated reactants, $\Delta(E+ZPE)$ values, has been calculated to lie in the -13.6 (IIIb) and -53.6 kcal mol^{-1} (IVa) range. Moreover, it is important to remark that the differences between relative energies calculated using B3LYP and CCSD(T) methodologies are smaller than 3 kcal mol^{-1} , i.e., less than 10% of the energetic stabilization of the binding process. The CO_2 capture implies a relevant decrease of the system entropy (the reaction moves from two reactants to one product); i.e., the entropic contribution to the free energy has an important effect, with the exoergicity of the process reduced by about 12 kcal mol^{-1} with respect to $\Delta(E+ZPE)$. Such exothermic processes may seem expected and surprising at the same time. The N_3^{3-} and CO_2 are electron rich and poor electron systems, respectively, and hence a strong and attractive interaction is expected between such nucleophilic and electrophilic systems. However, the formation of the $\text{Li}_3\text{N}_3\text{CO}_2$ compound also implies the distortion of the CO_2 linearity (reduction of stability around 75 kcal mol^{-1})⁴² and the π bond conversion of the sp -hybridized carbons, CO_2 , to the weaker sp^2 -hybridized carbons, NCO_2 .^{23,43} The fact that the CO_2 adsorption process takes place in not the most stable conformation of Li_3N_3 is an additional problem, but not an insurmountable one; in the literature^{44–46} examples have been reported of systems where the higher isomer was experimentally obtained before the global minimum structure.

In the three conformations with C_s symmetry (IIIa, IIIb, and IVa), the carbon dioxide and N_3^{3-} species occupy the same plane keeping the original planarity of structures III and IV. Moreover, the structures with the CO_2 bonded to the outer N_3^{3-} nitrogen atoms (IIIa and IVa) are seen to be much more stable (around 25 and 40 kcal mol^{-1} , respectively, $\Delta(E+ZPE)$ values) than IIIb, which shows the CO_2 attached to the central nitrogen atom. The remaining isomer, IIIc, shows a $\angle\text{NNNC}$ dihedral angle of 161.8° and the most important geometrical distortion with respect to the isolated reactant (III), with a relative stability of -36.4 kcal mol^{-1} .

Analyzing the geometrical parameters of the four organic compounds displayed in Figure 2, it is possible to establish a link between their relative stabilities and their N– CO_2 bond distances. The most stable conformation of $\text{Li}_3\text{N}_3\text{CO}_2$, IVa with a stability of -53.6 kcal mol^{-1} $\Delta(E+ZPE)$ value, shows the shortest N– CO_2 bond distance, 1.423 Å, while the less stable one, IIIb with -13.6 kcal mol^{-1} , presents the longest N– CO_2 bond distance, 1.751 Å. The two remaining structures, IIIa and IIIc, show an intermediate stabilization (-38.2 and -36.4 kcal mol^{-1}) and intermediate N– CO_2 bond distances (1.451 and 1.467 Å), in the above order.

The bonding process involving a second CO_2 molecule has been performed in a similar way by locating the second carbon dioxide around 2 Å of one of the remaining free (without a N– CO_2 bond) nitrogen atoms in the IIIa, IIIb, IIIc, and IVa systems, while considering also various orientations for CO_2 with respect to $\text{Li}_3\text{N}_3\text{CO}_2$. Then, the system has been fully optimized, with the structures having two carbon dioxides bonded to the N_3^{3-} species (IIIaa, IVaa, and IVab) selected and given in Figure 3 together with their relative stabilities relative to the isolated reactants (see also Table 2). It is important to remark that, in all other considered cases, the additional carbon dioxide does not bind to the N_3^{3-} structure and creates a van der Waals complex with $\text{Li}_3\text{N}_3\text{CO}_2$ or its capture implies the release of the formerly bonded CO_2 molecule; i.e., the system

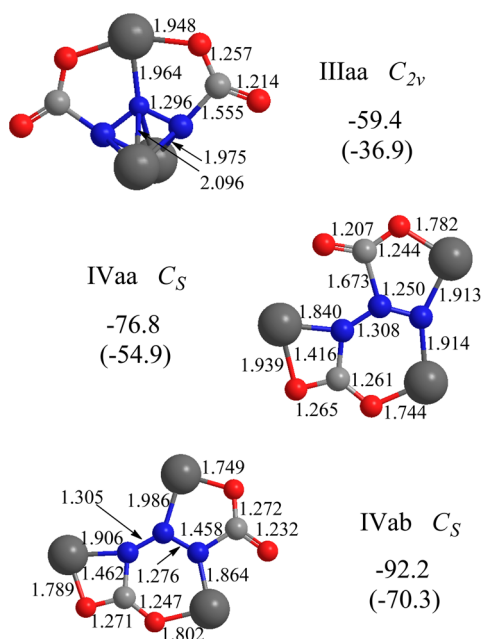


Figure 3. Structures of the organic compounds obtained from the interaction of the four $\text{Li}_3\text{N}_3\text{CO}_2$ structures obtained in this work (Figure 2) with another CO_2 at the CCSD(T)/aug-cc-pVTZ//B3LYP/aug-cc-pVTZ level of theory. The values are relative energies plus ZPE, with relative free energies given in parentheses, all in kcal mol⁻¹.

moves from one $\text{Li}_3\text{N}_3\text{CO}_2$ conformation to another, more stable one.

In Figure 3, the structure IIIaa is seen to show a C_{2v} symmetry and a computed relative stability of -59.4 kcal mol⁻¹, $\Delta(E+\text{ZPE})$ value. It has been obtained by adding a second carbon dioxide molecule to the external nitrogen atom of IIIa. Note that the first and second CO_2 captures imply stabilization processes of 38.2 and 21.2 kcal mol⁻¹ with respect to III and IIIa, respectively, showing that the bonding of a second CO_2 molecule has a smaller stabilization effect than the first. Moreover, the capture of a second CO_2 leads to a lengthening of the N– CO_2 bond by 0.104 Å (in agreement with the reduction of its relative stability).

From structure IVa, it is possible to generate two new structures (IVaa and IVab) with the CO_2 capture occurring at the central and external nitrogen atoms of IVa which show relative stabilities of -76.8 and -92.2 kcal mol⁻¹, respectively. These are comparable to the values reported for the capture of a CO_2 molecule by Li_3N .²⁴ As discussed above, the binding of a second CO_2 has a smaller stabilization effect than the first (23.3 and 38.6 kcal mol⁻¹ in IVaa and IVab vs 53.6 kcal mol⁻¹ in IVa). Another example of the relation between relative stabilities and N– CO_2 bond distances is conformation IVab, which shows shorter N– CO_2 bond distances than IVaa: 1.462 and 1.458 Å vs 1.416 and 1.673 Å.

To analyze in more detail the above issue, we correlate the relative stabilities divided by the number of CO_2 molecules bonded to Li_3N_3 , $\Delta(E+\text{ZPE})/N_{\text{CO}_2}$ in kcal mol⁻¹, and the average of the N– CO_2 bond distances, $\bar{d}_{\text{N}-\text{CO}_2}$ in Å, for the seven organic compounds studied in this work (see Figure 4). Although the R^2 value of 0.84 is not as high as one might ambition, there is a clear pattern between relative stabilities and N– CO_2 bond distances.

Finally, we study the binding of a third CO_2 molecule in the remaining free nitrogen atom for the IIIaa, IVaa, and IVab structures. In all cases, the additional carbon dioxide does not bind to the N_3^{3-} species or its capture implies the release of one of the two CO_2 molecules already bound to $\text{Li}_3\text{N}_3(\text{CO}_2)_2$.

4. CONCLUDING REMARKS AND PERSPECTIVE

We have studied the capture of both one and two carbon dioxide molecules by the four lowest energy structures of Li_3N_3 using the CCSD(T)/aug-cc-pVTZ//B3LYP/aug-cc-pVTZ methodology. Our results lead to the following conclusions. The binding of a CO_2 molecule is a very exoergic and irreversible process, but only possible if the Li_3N_3 conformer assumes a nonlinear N_3^{3-} form. Moreover, it occurs without any apparent energetic barrier. According to our calculations, it can yield four (three) different organic compounds with one (two) CO_2 molecule(s) bonded to the polynitrogen chain. The relative stabilities of these structures, $\Delta(E+\text{ZPE})$ values, with respect to the isolated reactants have been calculated to be in the -13.6 to -53.6 kcal mol⁻¹ (-59.4 to -92.2 kcal mol⁻¹) range for the binding of one (two) CO_2 . Thus, the binding of a second CO_2 has always a smaller stabilization effect than the first. Furthermore, a relation is apparent between the relative

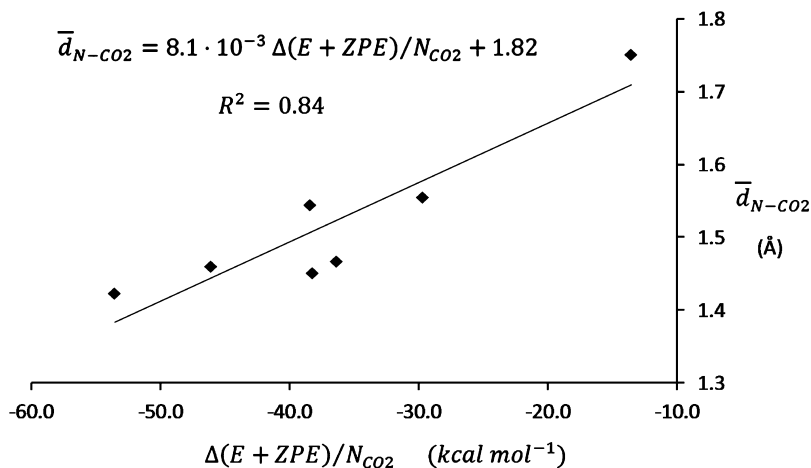


Figure 4. Relative stabilities divided by the number of CO_2 molecules bound to Li_3N_3 , $\Delta(E+\text{ZPE})/N_{\text{CO}_2}$ in kcal mol⁻¹, versus the average of the N– CO_2 bond distances, $\bar{d}_{\text{N}-\text{CO}_2}$ in Å, for the systems studied in this work.

stabilities of the seven new organic systems and their N–CO₂ bond distances: the shorter the N–CO₂ bond distance, the more stable the structure.

We hope that this work can motivate experimental research groups to design future experiments for the synthesis of new polynitrogen materials, e.g., Li₃N₃. The recent work of Murphy et al.²² with the synthesis of cyanofornate anion and its polarity switchable solvent system may have paved in this respect the way to novel and efficient CO₂ sequestrations. Additional work on new CO₂ complexes with anions showing solvent dependency behavior is in progress in our laboratory.

■ ASSOCIATED CONTENT

■ Supporting Information

Table S1 collects the energetics of the four lowest lying structures of Li₃N₃ calculated at the M06-2X/aug-cc-pVTZ and CAM-B3LYP/aug-cc-pVTZ levels. Table S2 (S3) contains the calculated harmonic vibrational frequencies and harmonic IR intensities and Raman scattering activities (N–CO₂ bond distances and bond orders) for the organic compounds obtained from Li₃N₃ + CO₂ and Li₃N₃ + 2CO₂. Figure S1 displays the relaxed potential energy surface scans along the N–CO₂ bond distance for the seven Li₃N₃CO₂ and Li₃N₃(CO₂)₂ compounds studied. Table S4 collects the Cartesian coordinates of all stationary points investigated in the present work. This material is available free of charge via the Internet at <http://pubs.acs.org>.

■ AUTHOR INFORMATION

Corresponding Authors

*E-mail: miqueltorrentsucarrat@gmail.com.

*E-mail: varandas@uc.pt.

Notes

The authors declare no competing financial interest.

■ ACKNOWLEDGMENTS

This work is supported by Fundação para a Ciência e a Tecnologia, Portugal (Contracts PTDC/CEQ-COM3249/2012 and PTDC/AAG-MAA/4657/2012). The support to the Coimbra Chemistry Centre through the project PEst-OE/QUI/UI0313/2014 is also gratefully acknowledged. We would also like to thank the reviewers for their comments and suggestions on this work.

■ REFERENCES

- (1) Broecker, W. S. Thermohaline Circulation, the Achilles Heel of our Climate System: Will Man-made CO₂ upset the Current Balance? *Science* **1997**, *278*, 1582–1588.
- (2) Hoffert, M. I.; Caldeira, K.; Benford, G.; Criswell, D. R.; Green, C.; Herzog, H.; Jain, A. K.; Khesghi, H. S.; Lackner, K. S.; Lewis, J. S.; et al. Advanced Technology Paths to Global Climate stability: Energy for a Greenhouse Planet. *Science* **2002**, *298*, 981–987.
- (3) Karl, T. R.; Trenberth, K. E. Modern Global Climate Change. *Science* **2003**, *302*, 1719–1723.
- (4) Kerr, R. A. Global Warming is Changing the World. *Science* **2007**, *316*, 188–190.
- (5) Inoue, T.; Fujishima, A.; Konishi, S.; Honda, K. Photoelectrocatalytic Reduction of Carbon-dioxide in Aqueous Suspensions of Semiconductor Powders. *Nature* **1979**, *277*, 637–638.
- (6) Takeda, H.; Koike, K.; Inoue, H.; Ishitani, O. Development of an Efficient Photocatalytic System for CO₂ Reduction using Rhenium(I) Complexes Based on Mechanistic Studies. *J. Am. Chem. Soc.* **2008**, *130*, 2023–2031.
- (7) Iizuka, K.; Wato, T.; Miseki, Y.; Saito, K.; Kudo, A. Photocatalytic Reduction of Carbon Dioxide over Ag Cocatalyst-Loaded ALA(4)-Ti(4)O(15) (A = Ca, Sr, and Ba) Using Water as a Reducing Reagent. *J. Am. Chem. Soc.* **2011**, *133*, 20863–20868.
- (8) Schaub, T.; Paciello, R. A. A Process for the Synthesis of Formic Acid by CO₂ Hydrogenation: Thermodynamic Aspects and the Role of CO. *Angew. Chem., Int. Ed.* **2011**, *50*, 7278–7282.
- (9) Wesselbaum, S.; vom Stein, T.; Klankermayer, J.; Leitner, W. Hydrogenation of Carbon Dioxide to Methanol by Using a Homogeneous Ruthenium-Phosphine Catalyst. *Angew. Chem., Int. Ed.* **2012**, *51*, 7499–7502.
- (10) Berkefeld, A.; Piers, W. E.; Parvez, M.; Castro, L.; Maron, L.; Eisenstein, O. Decamethylscandocinium-hydrido-(perfluorophenyl)-borate: Fixation and Tandem Tris(perfluorophenyl)-borane Catalysed Deoxygenative Hydrosilation of Carbon Dioxide. *Chem. Sci.* **2013**, *4*, 2152–2162.
- (11) Bontemps, S.; Sabo-Etienne, S. Trapping Formaldehyde in the Homogeneous Catalytic Reduction of Carbon Dioxide. *Angew. Chem., Int. Ed.* **2013**, *52*, 10253–10255.
- (12) LeBlanc, F. A.; Piers, W. E.; Parvez, M. Selective Hydrosilation of CO₂ to a Bis(silylacetel) Using an Anilido Bipyridyl-Ligated Organoscandium Catalyst. *Angew. Chem., Int. Ed.* **2014**, *53*, 789–792.
- (13) Zhang, S.; Kang, P.; Ubnoske, S.; Brennaman, M. K.; Song, N.; House, R. L.; Glass, J. T.; Meyer, T. J. Polyethylenimine-Enhanced Electrocatalytic Reduction of CO₂ to Formate at Nitrogen-Doped Carbon Nanomaterials. *J. Am. Chem. Soc.* **2014**, *136*, 7845–7848.
- (14) Rochelle, G. T. Amine Scrubbing for CO₂ Capture. *Science* **2009**, *325*, 1652–1654.
- (15) Puxty, G.; Rowland, R.; Attalla, M. Comparison of the Rate of CO₂ Absorption into Aqueous Ammonia and Monoethanolamine. *Chem. Eng. Sci.* **2010**, *65*, 915–922.
- (16) Wang, M.; Lawal, A.; Stephenson, P.; Sidders, J.; Ramshaw, C. Post-combustion CO₂ Capture with Chemical Absorption: A State-of-the-art Review. *Chem. Energy Res. Des.* **2011**, *89*, 1609–1624.
- (17) Luo, X. Y.; Guo, Y.; Ding, F.; Zhao, H. Q.; Cui, G. K.; Li, H. R.; Wang, C. M. Significant Improvements in CO₂ Capture by Pyridine-Containing Anion-Functionalized Ionic Liquids through Multiple-Site Cooperative Interactions. *Angew. Chem., Int. Ed.* **2014**, *53*, 7053–7057.
- (18) Schneider, S. B.; Frankovsky, R.; Schnick, W. High-Pressure Synthesis and Characterization of the Alkali Diazenide Li₂N₂. *Angew. Chem., Int. Ed.* **2012**, *51*, 1873–1875.
- (19) Olson, J. K.; Ivanov, A. S.; Boldyrev, A. I. All-Nitrogen Analogue of Ozone: Li₃N₃ Species. *Chem.—Eur. J.* **2014**, *20*, 6636–6640.
- (20) Hering, C.; von Langermann, J.; Schulz, A. The Elusive Cyanofornate: An Unusual Cyanide Shuttle. *Angew. Chem., Int. Ed.* **2014**, *53*, 8282–8284.
- (21) Zhang, X. Z.; Gross, U.; Seppelt, K. Fluorocarbonate, [FCO₂][−]: Preparation and Structure. *Angew. Chem., Int. Ed.* **1995**, *34*, 1858–1860.
- (22) Murphy, L. J.; Robertson, K. N.; Harroun, S. G.; Brosseau, C. L.; Werner-Zwanziger, U.; Moilanen, J.; Tuononen, H. M.; Clyburne, J. A. C. A Simple Complex on the Verge of Breakdown: Isolation of the Elusive Cyanofornate Ion. *Science* **2014**, *344*, 75–78.
- (23) Alabugin, I.; Mohamed, R. K. A CO₂ Cloak for the Cyanide Dagger. *Science* **2014**, *344*, 45–46.
- (24) Varandas, A. J. C. On Carbon Dioxide Capture: an Accurate Ab Initio Study of the Li₃N + CO₂ Insertion Reaction. *Comput. Theor. Chem.* **2014**, *1036*, 61–71.
- (25) Frisch, M. J.; Trucks, G. W.; Schlegel, H. B.; Scuseria, G. E.; Robb, M. A.; Cheeseman, J. R.; Scalmani, G.; Barone, V.; Mennucci, B.; Petersson, G. A. et al. *Gaussian09*; Gaussian, Inc.: Wallingford, CT, 2010.
- (26) Becke, A. D. Density-Functional Thermochemistry. 3. The Role of Exact Exchange. *J. Chem. Phys.* **1993**, *98*, 5648–5652.
- (27) Zhao, Y.; Truhlar, D. G. The M06 Suite of Density Functionals for Main Group Thermochemistry, Thermochemical Kinetics, Non-covalent Interactions, Excited States, and Transition Elements: Two New Functionals and Systematic Testing of Four M06-class

Functionals and 12 other Functionals. *Theor. Chem. Acc.* **2008**, *120*, 215–241.

(28) Yanai, T.; Tew, D. P.; Handy, N. C. A New Hybrid Exchange-correlation Functional using the Coulomb-attenuating Method (CAM-B3LYP). *Chem. Phys. Lett.* **2004**, *393*, 51–57.

(29) Dunning, T. H. Gaussian-basis Sets for use in Correlated Molecular Calculations. 1. The Atoms Boron Through Neon and Hydrogen. *J. Chem. Phys.* **1989**, *90*, 1007–1023.

(30) Kendall, R. A.; Dunning, T. H.; Harrison, R. J. Electron-affinities of the 1st-row Atoms Revisited - Systematic Basis-sets and Wave-functions. *J. Chem. Phys.* **1992**, *96*, 6796–6806.

(31) Schuchardt, K. L.; Didier, B. T.; Elsethagen, T.; Sun, L. S.; Gurumoorthi, V.; Chase, J.; Li, J.; Windus, T. L. Basis Set Exchange: A Community Database for Computational Sciences. *J. Chem. Inf. Model.* **2007**, *47*, 1045–1052.

(32) Cizek, J. On the use of the cluster expansion and the technique of diagrams in calculations of correlation effects in atoms. *Adv. Chem. Phys.* **1969**, *14*, 35–89.

(33) Pople, J. A.; Krishnan, R.; Schlegel, H. B.; Binkley, J. S. Electron correlation theories and their application to the study of simple reaction potential surfaces. *Int. J. Quantum Chem.* **1978**, *14*, 545–560.

(34) Barlett, R. J. Coupled-cluster approach to molecular structure and spectra: a step toward predictive quantum chemistry. *J. Phys. Chem.* **1989**, *93*, 1697–1708.

(35) Varandas, A. J. C. Accurate Determination of the Reaction Course in $\text{HY}_2 \rightleftharpoons \text{Y} + \text{YH}$ ($\text{Y} = \text{O}, \text{S}$): Detailed Analysis of the Covalent- to Hydrogen-Bonding Transition. *J. Phys. Chem. A* **2013**, *117*, 7393–7407.

(36) Viegas, L. P.; Varandas, A. J. C. Coupled-Cluster Reaction Barriers of $\text{HO}_2 + \text{H}_2\text{O} + \text{O}_3$: An Application of the Coupled-Cluster//Kohn–Sham Density Functional Theory Model Chemistry. *J. Comput. Chem.* **2014**, *35*, 507–517.

(37) Varandas, A. J. C. Odd-Hydrogen: An Account on Electronic Structure, Kinetics, and Role of Water in Mediating Reactions with Atmospheric Ozone. Just a Catalyst or Far Beyond? *Int. J. Quantum Chem.* **2014**, *114*, 1327–1349.

(38) Mayer, I.; Salvador, P. Overlap populations, bond orders and valences for ‘fuzzy’ atoms. *Chem. Phys. Lett.* **2004**, *383*, 368–375.

(39) Becke, A. D. A Multicenter Numerical-Integration Scheme For Polyatomic-Molecules. *J. Chem. Phys.* **1988**, *88*, 2547–2553.

(40) Matito, E.; Solà, M.; Salvador, P.; Duran, M. Electron sharing indexes at the correlated level. Application to aromaticity calculations. *Faraday Discuss.* **2007**, *135*, 325–345.

(41) Mayer, I.; Salvador, P. Program “FUZZY”, Version 1.00; Girona, October 2003.

(42) Alabugin, I. V.; Gold, B.; Shatruk, M.; Kovnir, K. Comment on “Single-Crystal X-ray Structure of 1,3-Dimethylcyclobutadiene by Confinement in a Crystalline Matrix”. *Science* **2014**, *330*, 1047.

(43) Nicolaides, A.; Borden, W. T. Ab initio Calculations of the Relative Strengths of the π -bonds in Acetylene and Ethylene and of their Effect on the Relative Energies of π -bond Addition-reactions. *J. Am. Chem. Soc.* **1991**, *113*, 6750–6755.

(44) Sekiguchi, A.; Yatabe, T.; Kabuto, C.; Sakurai, H. Chemistry of Organosilicon Compounds. 303. The “Missing” Hexasilaprismane: Synthesis, X-ray Analysis, and Photochemical Reactions. *J. Am. Chem. Soc.* **1993**, *115*, 5853–5854.

(45) Abersfelder, K.; White, A. J. P.; Berger, R. J. F.; Rzepa, H. S.; Scheschkewitz, D. A Stable Derivative of the Global Minimum on the Si_6H_6 Potential Energy Surface. *Angew. Chem., Int. Ed.* **2011**, *50*, 7936–7939.

(46) Ivanov, A. S.; Boldyrev, A. I. $\text{Si}_{6-n}\text{C}_n\text{H}_6$ ($n = 0–6$) Series: When Do Silabenzenes Become Planar and Global Minima? *J. Phys. Chem. A* **2012**, *116*, 9591–9598.